archives
of thermodynamics
Vol. **33**(2012), No. 1, 67–86
DOI: 10.2478/v10173-012-0003-2

Models for water steam condensing flows

WŁODZIMIERZ WRÓBLEWSKI*
SŁAWOMIR DYKAS
TADEUSZ CHMIELNIAK

Silesian University of Technology, Institute of Power Engineering and Turbomachinery, Konarskiego 18, 44-100 Gliwice, Poland

Abstract The paper presents a description of selected models dedicated to steam condensing flow modelling. The models are implemented into an in-house computational fluid dynamics code that has been successfully applied to wet steam flow calculation for many years now. All models use the same condensation model that has been validated against the majority of available experimental data. The state equations for vapour and liquid water, the physical model as well as the numerical techniques of solution to flow governing equations have been presented. For the single-fluid model, the Reynolds-averaged Navier-Stokes equations for vapour/liquid mixture are solved, whereas the two-fluid model solves separate flow governing equations for the compressible, viscous and turbulent vapour phase and for the compressible and inviscid liquid phase. All described models have been compared with relation to the flow through the Laval nozzle.

Keywords: Wet steam; Condensing flow models; Laval nozzle

Nomenclature

a_w	–	water activity in a solution
c	–	speed of sound, m/s
C_c	–	Cunningham slip correction factor
e	–	specific internal energy, J/m^3
E	–	specific total energy, J/m^3
h	–	specific enthalpy, J/kg
H	–	specific total enthalpy, J/kg

*Corresoponding author. E-mail address: wlodzimierz.wroblewski@polsl.pl

J – nucleation rate, $1/(\mathrm{m}^3\mathrm{s})$
l_s – mean free path, m
k – Boltzmann constant ($1.3804{\cdot}10^{-23}$), J/K
Kn – Knudsen number, $\mathrm{Kn} \equiv l_s/2r$
M – Mach number
M_l – molality, mol/kg
m – mass of a water molecule ($2.99152{\cdot}10^{-26}$), kg
$\dot{m}$ – mass flux, kg/s
n_{het} – droplet number per volume (heterogeneous), $1/\mathrm{m}^3$
n – droplet number per mass (homogeneous), 1/kg
p – static pressure, Pa
r – droplet radius, m
R – individual gas constant (461.52 for vapour), J/(kgK)
Re – Reynolds number
t – time, s
T – static temperature, K
u – velocity, m/s
x – spatial variable, m
y – mass fraction of the liquid phase
z – compressibility coefficient

Greek symbols

α – volume fraction
β – correction factor
Γ – mass source, $\mathrm{kg}/(\mathrm{m}^3\,\mathrm{s})$
γ – isentropic exponent
δ_{ji} – Kronecker delta
λ – heat conductivity, W/(mK)
μ – molecular viscosity, Pa s
ρ – density, kg/m^3
σ – surface tension, N/m
τ – shear stress tensor, N/m

Subscripts

0 – total
het – heterogeneous
int – interfacial
i, j – indices
L – left
l – liquid phase
m – mixture
o – surface
R – right
S – saturated
v – vapour phase
w – water
$'$ – saturated water
$''$ – dry saturated vapour
$*$ – critical parameter, parameters from 'star' region

1 Introduction

The low-pressure turbine blades are one of the most important components in the overall steam turbine design. A fully developed 3D stage flow analysis can provide an optimum blade profile capable of minimizing the losses from shock waves resulting from the supersonic flow. The accuracy of the modern 3D analysis as a prediction tool has improved considerably and it can now account for non-equilibrium condensation flows with different steam wetness conditions and phase change variations [1,2].

The steam temperature in low-pressure turbines decreases due to expansion. In turbines of large output the superheated vapour usually crosses the saturation line in penultimate stages. At least the last two stages of the low-pressure turbine operate in the two-phase region producing much more than 10% of the total output. The presence of the liquid phase within the turbine causes thermodynamic losses (caused by the internal heat transfer within the fluid), aerodynamic losses (losses that occur due to the interaction of the fluid with the walls and caused by aerodynamic shocks) and mechanical losses or erosion (droplet impingement on the blades damages the steam turbine blades). Therefore, any decrease in them is worth striving for.

There are two main kinds of numerical models of the wet steam flow with condensation which can be applied to the flow field modelling in low-pressure (LP) stages. One includes the single-fluid model (SFM) and is called a no-slip model. The other is a two-fluid model (TFM) taking into account the velocity slip between the vapour and the liquid phase.

Modelling steam condensation has been investigated in thermodynamic and gas dynamic aspects by numerous authors for many years now [3–5]. A lot of experimental data for the flow in the Laval nozzle and 2D blade cascades have been contributed to the validation of the computational fluid dynamics (CFD) methods with implemented various condensation models [1,3,4], but mainly SFM models. These models seemed to be well-suited for modelling the wet steam flow in real turbine stages [6,7] to determine both thermodynamic and aerodynamic losses. However, in order to predict mechanical losses, especially the trajectory of liquid droplets and their possible impingement on the blade surface, a two-fluid model has to be applied, in which the velocity slip between the phases is taken into account. It allows better understanding the processes of the blade surface deterioration. Two-fluid models for such type of flow are much more complicated and, consequently, much less popular.

The aim of this paper is to present models for the wet steam flow field

prediction. These models are implemented into an in-house CFD code [14] used for many years at the Institute of Power Engineering and Turbomachinery of the Silesian University of Technology in Gliwice for engineering applications.

2 Physical model

Steam with high velocity in LP stages achieves a supercooled state and then the subcooled vapour loses its latent heat. During that process liquid droplets with small diameters are formed. Next, depending on the thermodynamic conditions these small droplets grow or vanish. Hence, the numerical algorithm modelling such flow must solve the equations governing the compressible flow supplemented by the real gas equation of state, and the algorithm should include additional relations describing phase transitions.

It was assumed in the presented models that the two phases are governed by the same pressure:

$$p = p_v = p_l \ , \tag{1}$$

where indices v and l denote the liquid and vapour phase, respectively. The following relationships connect the liquid and the vapour phase:

$$\begin{array}{rcl} \alpha & = & \dfrac{V_l}{V_m} \ , \\ \rho_m & = & (1-\alpha)\,\rho_v + \alpha\rho_l \ , \\ h_m & = & (1-y)\,h_v + y h_l \ , \\ y & = & \alpha\dfrac{\rho_l}{\rho_m} \ , \end{array} \tag{2}$$

where α is volume fraction and y is the mass fraction of liquid phase, and $V_{l,}, V_m$ are respectively the volume of liquid phase and mixture. The density of the mixture ρ_m, is a function of vapour density ρ_v, liquid density ρ_l, and volume fraction α. The enthalpy of mixture h_m, is determined in a similar way, where h_ν and h_l are specific enthalpy of vapour and liquid. Mass fraction y depends on the volume fraction as well as on the ratio between the liquid and the mixture density, and for the presented problem has a value by approx. 10^3 higher than the volume fraction.

2.1 Equation of state for vapour

There are many forms of real gas equations of state for steam known from literature. At the moment, the most accurate and widely used and the

most recommended for industrial use is the "IAPWS Industrial Formulation 1997" (IAPWS-IF97). It consists of a set of equations for different regions. The basic equation for each region is a fundamental equation for the specific Gibbs free energy. This equation has a very complicated form and is practically useless for a direct application into CFD codes. In the presented in-house CFD code the 'local' real gas state equation was used in a form similar to the virial equation of state with one virial coefficient [2]:

$$\frac{p}{RT_v\rho_v} = z\left(T_v, \rho_v\right) = A(T_v) + B(T_v)\rho_v \ , \tag{3}$$

where p, T_v are pressure and temperature of vapour, respectively, $R = 461.5$ J/(kg K) is the gas constant, z stands for the compressibility coefficient and polynomials $A(T)$, $B(T)$ are defined as:

$$A(T) = a_0 + a_1 T + a_2 T^2 \ ,$$

$$B(T) = b_0 + b_1 T + b_2 T^2 \ .$$

Coefficients a_i, b_i ($i = 0,1,2$) of polynomials $A(T)$ and $B(T)$ are the functions of temperature only, and they are calculated from an approximation of the thermodynamic properties of steam following the IAPWS-IF97.

Due to its simple form, the solution to the flow governing equations is obtained relatively fast, but it is still necessary to solve the non-linear equations to determine the primitive variables from the conservatives ones. The applied simple mathematical form of a real gas equation of state (EOS) can be very accurate, but only for a limited range of parameters. The rest of the thermodynamic properties of the vapour phase are calculated on the basis of the applied state equation (3).

2.2 Equation of state for liquid

While considering water under the conditions close to the saturation line for pressure smaller than 1 bar, the IAPWS-IF97 can be used as well, where the liquid water properties like temperature, density, enthalpy and speed of sound c can be determined from the following functions:

$$\begin{aligned} T_l &= T_l\left(p, h_l\right) \ , \\ \rho_l &= \rho_l\left(p, T_l\right) \ , \\ h_l &= h_l\left(p, T_l\right) \ , \\ c_l &= c_l\left(p, T_l\right) \ . \end{aligned} \tag{4}$$

The functions in Eqs. (4) in the considered region of liquid water are very sensitive, and even a minute change of parameters can bring about a significant change of their value. It is of course very inconvenient for the numerical algorithm solving the flow governing equations.

2.3 Non-equilibrium condensation model

2.3.1 Homogeneous condensation

The nucleation model presented in this study is a homogeneous nucleation. In this kind of nucleation, condensation occurs without any impurity or surfaces. In the supersonic region, if the flow is heated by the latent heat of the condensation process, its velocity decreases and its pressure increases. Therefore, a condensation shock (or rise in pressure) occurs, which increases the flow entropy producing local losses.

In the presented models, the homogeneous condensation phenomenon is modelled on the basis of the classical nucleation [8] and the continuous droplet growth model [9]. The nucleation rate, i.e. the number of supercritical droplets produced per mass unit of vapour per time unit, is calculated from the relation obtained according to the classical nucleation theory. This relation has been derived by an assumption of a thermodynamic equilibrium between critical droplets and vapour:

$$J_{hom} = C\sqrt{\frac{2\sigma}{\pi}} m^{-3/2} \frac{\rho_v}{\rho_l} \exp\left(-\beta \frac{4\pi r^{*2}\sigma}{3kT_v}\right) , \tag{5}$$

where σ is the surface tension, m is the mass of a water molecule, β is the correction factor coefficient, k is the Boltzmann constant and C is the non-isothermal correction factor proposed by Kantrowitz [10]

$$C = \left[1 + 2\frac{\gamma - 1}{\gamma + 1}\frac{h_v - h_l}{RT_v}\left(\frac{h_v - h_l}{RT_v} - \frac{1}{2}\right)\right]^{-1} , \tag{6}$$

because the isothermal model assumption does not apply to vapour, where γ is isentropic exponent. The correction factor applied in the presented calculations is $\beta = 1$.

The radius of critical clusters $r*$ for the applied real gas EOS (Eq. (3)) has a form, which differs from the known relation for the ideal gas:

$$r^* = \frac{2\sigma}{\rho_l(f(p_v) - f(p_s)) - (p_v - p_s)} , \tag{7}$$

where:

$$f(p) = \frac{d_A}{2}\ln p + \sqrt{d_A^2 + 4pd_B} - \frac{d_A}{2}\ln\left(\frac{1+\frac{\sqrt{d_A^2+4pd_B}}{d_A}}{1-\frac{\sqrt{d_A^2+4pd_B}}{d_A}}\right) ,$$
$$d_A = A(T)RT ,$$
$$d_B = B(T)RT ,$$

in which p_s stands for saturated pressure.

The further behaviour of the critical droplets can be described by the suitable droplet growth law. Once the droplets are formed, they increase in size as vapour molecules condense on their surfaces. The energy released in condensation leads to a rise in temperature of the droplets, and hence, droplets become hotter than the surrounding vapour during condensation. The droplet growth is thus governed mainly by the mass transfer towards a droplet and energy flux away from it. In pure vapour, however, due to the release of a very high latent heat in the rapid condensation zone, the droplet growth is dominated by the thermal transfer rate.

Knudsen number, Kn, plays a key role in the coefficient of the heat transfer due to a wide range of the radii of droplets. Knudsen number expresses the ratio of the mean free path of vapour molecules to the droplet diameter (Kn$= l_s/2r$).

The size of droplets for vapour under low pressure is much smaller than the mean free path of vapour molecules. Therefore, the growth of the droplets should be governed by considering the molecular and macroscopic transport process (Hertz-Knudsen model). The problems with the choice of the condensation and accommodation coefficients make the application of the Hertz-Knudsen model very difficult for calculations. This problem can be avoided by using Gyarmathy's droplet growth model, which takes into account the diffusion of vapour molecules through the surrounding vapour as well as the heat and mass transfer, and the influence of capillarity:

$$\frac{dr}{dt} = \frac{1}{\rho_l}\frac{\lambda_v}{(1+3.18\mathrm{Kn})}\frac{r-r^*}{r^2}\frac{T_s-T_v}{h_v-h_l} , \tag{8}$$

where r is the droplet radius, T_s is the saturation temperature and λ_v is the thermal conductivity of the vapour phase.

2.3.2 Heterogeneous condensation

In the heterogeneous condensation model the nucleation process is neglected. The existence of foreign solid particles favours the nucleation, mainly due

to the diminished thermodynamic barrier (compared to the homogeneous nucleation). The heterogeneous nucleation is rapid and has negligible influence on the results obtaining for expansion processes discussed below. This assumption enables to eliminate droplet number governing equation for heterogeneous droplets. The droplets growth on the particle impurities, which are assumed to be spherical with the given initial mean radius and concentration in mass unit, is modeled according to the same droplets growth law, Eq. (8).

The model of heterogeneous condensation on soluble particles is based on the work [11]. For heterogeneous condensation model on soluble particles (usually NaCl) the physical properties of steam have to be changed, because we do not deal with pure vapour but with the solution of the vapour and e.g. NaCl. In this case the saturated pressure and surface tension have to be corrected:

$$\begin{aligned} &p_{solution}(T_v) = a_w p_s(T_v) \ , \\ &\sigma = \sigma_o\,(T) + B\,M_l \ , \end{aligned} \tag{9}$$

where a_w represents the water activity and σ_o is a surface tension for the pure steam and water, M_l is molality and $B = 1.62 \cdot 10^{-3}$ N kg/(m mol) is a constant for NaCl.

2.4 Interfacial exchange terms

In the presented models the phase change is represented by two mass sources, according to the relations:

$$\begin{aligned} &\Gamma_1 = m_l^* J = \tfrac{4}{3}\pi\rho_l r^{*3} J \ , \\ &\Gamma_2 = 4\pi\rho_l\rho_m n r^2 \frac{dr}{dt} \ , \\ &\Gamma_{het} = 4\pi\rho_l\rho_m n_{het} r_{het}^2 \frac{dr_{het}}{dt} \ , \end{aligned} \tag{10}$$

where Γ_1 is the mass source of critical droplets of the mass created due to the nucleation process, and Γ_2, Γ_{het} is the mass condensation rate of all droplets per volume unit of the two-phase mixture [kg/(m^{3}s)] for homogeneous and heterogeneous condensation respectively, and J stand for nucleation rate, and m_l^* is the mass of a critical droplet.

2.5 Drag force

Taking account of the drag force in momentum equations for the TFM model is crucial for the correct prediction of the velocity field. Omission of

it for very small droplets in the transonic flow can lead to their excessive slowdown. For smaller Reynolds numbers, the molecular viscous forces have to be considered. Under the laminar flow conditions of the droplets ($\mathrm{Re} = \frac{\rho\left(u_{vj}-u_{lj}\right)2r}{\mu} < 1$) the molecular viscous forces dominate, and the inertial forces can be omitted. According to the Stokes law, the drag force can be written as:

$$F_{Dj} = -\frac{6\pi\mu r}{C_c}\frac{1}{V_m}\left(u_{vj}-u_{lj}\right) = -\frac{\frac{9}{2}\frac{\mu\alpha}{r^2}}{C_c}\left(u_{vj}-u_{lj}\right) \ , \tag{11}$$

where u_{vj} and u_{lj} are velocity components of the vapour and liquid, respectively, r is radius of the droplet, and μ is dynamic viscosity. An important assumption in the derivation of the Stokes law is that the relative velocity of the gas at the surface of the droplet is zero. This assumption does not hold for small droplets whose size approximates the mean free path of the vapour ($\mathrm{Kn} \gtrsim 1$). For this reason, the Stokes law has to be corrected with the empirical Cunningham slip correction factor:

$$C_c = 1 + 2\mathrm{Kn}\left(1.257 + 0.4\mathrm{e}^{-1.1/2\mathrm{Kn}}\right) \ . \tag{12}$$

Factor C_c depends on the ratio of the mean free path to the particle diameter and thereby also on the Knudsen number.

2.6 Governing equations for single-fluid model

A typical approach used for the analysis of two-phase flows is a mixture model, i.e. the individual fluid phases are assumed to behave as a flowing mixture described in terms of the mixture properties. The applied single-fluid model consists the mass, momentum and energy equations for a vapour/liquid mixture, two equations describing the formation and growth of the liquid phase occurred due to the homogeneous condensation:

$$\begin{aligned}
&\frac{\partial\rho_m}{\partial t} + \frac{\partial\left(\rho_m u_{mj}\right)}{\partial x_j} = 0 \ , \\
&\frac{\partial\left(\rho_m u_{mi}\right)}{\partial t} + \frac{\partial\left(\rho_l u_{mj}u_{mi} + p\delta_{ji}\right)}{\partial x_j} - \frac{\partial\tau_{ji}}{\partial x_j} = 0 \ , \\
&\frac{\partial\left(\rho_m E_m\right)}{\partial t} + \frac{\partial\left(\rho_m u_{mj}H_m\right)}{\partial x_j} + \frac{\partial\left(q_j - u_{mj}\tau_{ji}\right)}{\partial x_j} = 0 \ , \\
&\frac{\partial\left(\rho_m y\right)}{\partial t} + \frac{\partial\left(\rho_m u_{mj}y\right)}{\partial x_j} = \Gamma_1 + \Gamma_2 \ , \\
&\frac{\partial\left(\rho_m n\right)}{\partial t} + \frac{\partial\left(\rho_m u_{mj}n\right)}{\partial x_j} = J
\end{aligned} \tag{13}$$

and one for heterogeneous condensation:

$$\frac{\partial\left(\rho_m y_{het}\right)}{\partial t}+\frac{\partial\left(\rho_m u_{mj} y_{het}\right)}{\partial x_j}=\Gamma_{het}\ ,$$

where:

$$E_m=h_m-\frac{p}{\rho_m}+\frac{1}{2}u_{mj}u_{mj}$$

is the specific total internal energy of the mixture, H_m the specific total enthalpy of the mixture, δ_{ji}, τ_{ji} are the Kronecker delta and shear stress tensor, respectively, n denotes the droplet number per mass, and x_j represents the spatial variable.

Pressure p has to be calculated from the relation for the total energy of mixture:

$$\begin{aligned}E_m-h_v(p,\rho_v)(1-y-y_{het})-h_l(p)(y+y_{het})+\\ +\frac{p}{\rho_m}-\frac{1}{2}u_{mj}u_{mj}=0\ .\end{aligned}\tag{14}$$

The relation for pressure is of course non-linear due to the non-linear form of the applied equations of state for vapour and liquid (Eq. (3)), and is solved by means of the Newton iteration method.

In this model, the volume of the condensate is neglected. Thus, the density of the vapour phase is calculated from the mixture density and the wetness fraction only. Next, knowing the pressure and the vapour density, the temperature of the vapour phase is calculated from state equation, Eq. (3). The liquid temperature is calculated from the relation proposed in [9]:

$$T_l=T_s(p)-\left[T_s(p)-T_v\right]\frac{r^*}{r}=T_s(p)-\Delta T\frac{r^*}{r}\ .\tag{15}$$

2.7 Governing equations for two-fluid model

In the considered two-fluid model, homogeneous condensation will only be taken into account and separate sets of the governing equation for the vapour and liquid phases have been used. For the vapour phase they can

be written as follows:

$$\begin{aligned}
&\frac{\partial\left(\rho_v\left(1-\alpha\right)\right)}{\partial t}+\frac{\partial\left(\rho_v\left(1-\alpha\right)u_{vj}\right)}{\partial x_j}=-\Gamma_1-\Gamma_2\ ,\\
&\frac{\partial\left(\rho_v\left(1-\alpha\right)u_{vi}\right)}{\partial t}+\frac{\partial\left(\rho_v\left(1-\alpha\right)u_{vj}u_{vi}+(1-\alpha)p\delta_{ij}\right)}{\partial x_j}-\\
&\qquad+\frac{\partial\left(\left(1-\alpha\right)\tau_{ji}\right)}{\partial x_j}=-\Gamma_2 u_{int\,j}-F_{Dj}\ ,\\
&\frac{\partial\left(\rho_v\left(1-\alpha\right)E_v\right)}{\partial t}+\frac{\partial\left(\rho_v\left(1-\alpha\right)u_{vj}H_v\right)}{\partial x_j}+\\
&\quad+\frac{\partial\left(\left(1-\alpha\right)q_{vj}-\left(1-\alpha\right)u_{vi}\tau_{ji}\right)}{\partial x_j}=-\Gamma_2(H_{vint}-L)\ ,
\end{aligned}\tag{16}$$

where

$$E_v=h_v-\frac{p}{\rho_v}+\frac{1}{2}u_{vj}u_{vj}$$

is the specific total internal energy of the vapour, H_v is the specific total enthalpy of the vapour, and the subscript *int* indicates the interfacial location.

The liquid phase is in the form of a fog composed of small droplets. Therefore the authors have decided to use an inviscid form of the governing equations for the liquid phase:

$$\frac{\partial\left(\rho_l\alpha\right)}{\partial t}+\frac{\partial\left(\rho_l\alpha u_{lj}\right)}{\partial x_j}=\Gamma_1+\Gamma_2\ ,$$

$$\begin{aligned}
&\frac{\partial\left(\rho_l n\right)}{\partial t}+\frac{\partial\left(\rho_l n u_{lj}\right)}{\partial x_j}=J\ ,\\
&\frac{\partial\left(\rho_l\alpha u_{li}\right)}{\partial t}+\frac{\partial\left(\rho_l\alpha u_{lj}u_{li}+\alpha p\delta_{ij}\right)}{\partial x_j}=\Gamma_2 u_{int\,j}+F_{Dj}\ ,\\
&\frac{\partial\left(\rho_l\alpha E_l\right)}{\partial t}+\frac{\partial\left(\rho_l\alpha u_{lj}H_l\right)}{\partial x_j}=\Gamma_2 H_{lint}\ ,
\end{aligned}\tag{17}$$

where

$$E_l=h_l-\frac{p}{\rho_l}+\frac{1}{2}u_{lj}u_{lj}$$

is the specific total internal energy of the liquid and H its total enthalpy.

In Eqs. (16) and (17) $u_{int\,j}$ represents the interface velocity components and is calculated from relation:

$$u_{int\,j}=\frac{\rho_l u_{lj}\alpha+\rho_v u_{vj}\left(1-\alpha\right)}{\rho_m}\tag{18}$$

and $H_{l\,int}$, $H_{v\,int}$ are the total enthalpies for liquid and vapour, respectively, which are associated with the interphase mass transfer and calculated, assuming saturated conditions, in the following way:

$$\begin{aligned} H_{l\,int} &= h'(p) + u_{int\,j} u_{lj} - \tfrac{1}{2} u_{lj} u_{lj} \ , \\ H_{v\,int} &= h''(p) + u_{int\,j} u_{vj} - \tfrac{1}{2} u_{vj} u_{vj} \ , \end{aligned} \tag{19}$$

where superscripts next to specific enthalpy symbol indicate the saturated water and the dry saturated vapour.

In order to determine the primitive variables from the conservative ones used in the governing equations, the system of non-linear equations has to be solved:

$$\begin{aligned} &\frac{1}{\rho_m} - \left(\frac{1-y}{\rho_v} + \frac{y}{\rho_l} \right) = 0 \ , \\ &e_v - \left(h_v - \frac{p}{\rho_v} \right) = 0 \ , \\ &e_l - \left(h_l - \frac{p}{\rho_l} \right) = 0 \ , \end{aligned} \tag{20}$$

where e_v, e_l are the specific internal energy for vapour and liquid, respectively. The unknowns in these equations are p, h_v and h_l, while the remaining values:

$$\begin{aligned} \rho_m &= \left[(1-\alpha)\, \rho_v \right] + \left[\alpha \rho_l \right] \ , \\ y &= \frac{\left[\alpha \rho_l \right]}{\rho_m} \ , \\ e_v &= \frac{\left[(1-\alpha)\, \rho_v E_v \right]}{\left[(1-\alpha)\, \rho_v \right]} - \frac{1}{2} \left(\frac{\left[(1-\alpha)\, \rho_v u_{vi} \right]}{\left[(1-\alpha)\, \rho_v \right]} \right)^2 \ , \\ e_l &= \frac{\left[\alpha \rho_l E_l \right]}{\left[\alpha \rho_l \right]} - \frac{1}{2} \left(\frac{\left[\alpha \rho_l u_{li} \right]}{\left[\alpha \rho_l \right]} \right)^2 \end{aligned} \tag{21}$$

are constants calculated from the conservative variables (included in square brackets) obtained from Eqs. (16) and (17) after each iteration step. The phase densities are the functions of pressure and corresponding enthalpies and are calculated from the state equations for vapour and liquid water in accordance with the IAPWS-IF97 standard. Water temperature is calculated from the state equation for liquid water Eq. (4) in function of pressure and specific enthalpy. The set of non-linear equations (20) is solved by means of the Newton-Raphson method.

3 Numerical model

Both described models have been implemented into the in-house CFD code [14]. The numerical simulation is based on the time dependent 3D RANS equations. The "local" real gas equation of state, nonlinear relations for liquid water and the condensation theory are the closure relations for the applied flow governing equations.

The system of governing equations was discretized on a multi-block structured grid using the finite volume method, and integrated in time using an explicit Runge-Kutta method. An upwind scheme was used with the one-dimensional Riemann solver for the real gas equation of state. Because the exact solution to the Riemann problem is computationally expensive, an approximate Riemann solver was used. The acoustic approximation of the Riemann problem applied for vapour belongs to the flux difference splitting (FDS) group, where the primitive variables are estimated. The solver assumes weak variations across the left- and right-facing. To this end, the following mass flux can be defined:

$$m^* = \frac{c_L + c_R}{2} \frac{\rho_{vL} + \rho_{vR}}{2} \,, \tag{22}$$

where the subscripts L and R indicate the left and right state of the Riemann problem, respectively, and c is the speed of sound of the vapour phase. The parameters in "star" states L^* and R^* are obtained as the solution of the Riemann problem from the relations:

$$\begin{aligned}
p^* &= p_L^* = p_R^* = \frac{p_L + p_R}{2} + m^* \frac{u_{vL} - u_{vR}}{2} \,, \\
u^* &= u_L^* = u_R^* = \frac{u_{vL} + u_{vR}}{2} + \frac{p_L - p_R}{2m^*} \,, \\
\rho_L^* &= \rho_{vL} + \frac{m^* \left(u_{vL} - u^*\right)}{c_L^2} \,, \\
\rho_R^* &= \rho_{vR} + \frac{m^* \left(u^* - u_{vR}\right)}{c_R^2} \,.
\end{aligned} \tag{23}$$

The general structure of the Riemann problem for the liquid phase consists of shock waves and/or rarefaction waves in the $u-c$ and $u+c$ characteristic fields, and contact discontinuities u.

Acoustic approximation, Eq. (23), cannot be applied for the liquid phase. Therefore, a simple linearization of the Riemann invariants leads

to the linear algebraic system for state L^*:

$$\begin{array}{lcl} c_{lL}^2\left(\rho_{lL}-\rho_{lL}^*\right)-\left(p^*-p_L\right) & = & 0\,, \\ \rho_{lL}c_{lL}\left(u_l^*-u_{lL}\right)+\left(p^*-p_L\right) & = & 0\,, \\ \rho_{lR}c_{lR}\left(u_l^*-u_{lR}\right)-\left(p^*-p_R\right) & = & 0\,, \end{array} \tag{24}$$

which can be easily solved for u_l^*, ρ_{lL}^*, and p^*. An analogical system of equations can be defined between state R^* and R in order to find ρ_{lR}^*. Such assumption makes it possible to avoid using a complicated state equation for water to find primitive variables. Next, having the primitive variables from the Riemann problem, the fluxes can be calculated. The MUSCL technique is implemented to approach the TVD scheme with the flux limiter to avoid oscillations.

4 Results

The main intention of this work is to give an overview and to compare the presented models together. Validation of the SFM model has already been presented in previous works [2,13]. The calculations are carried out for all models. To model the condensing steam flow, the geometry of the arc Laval nozzle, with the radius of the wall curvature of 584 mm and the critical throat height of 60 mm, is assumed. The following boundary conditions at the inlet are set to: $p_0 = 78\ 390$ Pa, $T_0 = 380.55$ K. The geometry of the nozzle and the boundary conditions correspond to those in Barschdorff's experiment [12]. The outlet from the nozzle is supersonic. The inviscid flow model is applied for calculations.

4.1 Single-fluid model versus two-fluid model

Figures 1–4 show the comparison of the main flow parameters important in the case of steam flows with the nucleation process and the growth of liquid droplets. The static pressure distributions along the nozzle (Figs. 1 and 2) show a proper modelling of the place of condensation by means of both models. In the case of the TFM model, the condensation wave is smoother than in the case of the SFM model. The static temperature distributions for the liquid and the vapour phase have a very similar character. For the SFM model, the liquid temperature is calculated from Eq. (15), whereas for the TFM it is obtained from the governing equations for the liquid phase.

The SFM presented in this work underestimates the droplet radii. It was presented by Wroblewski *et al.* [13] that the radii of the droplets were

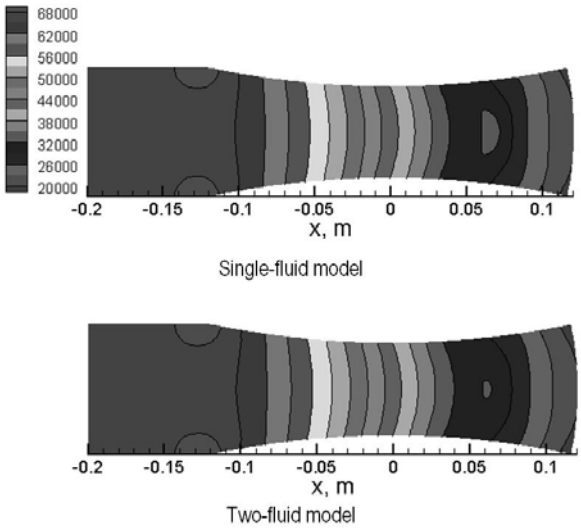

Figure 1. Static pressure distributions along the nozzle (2D view).

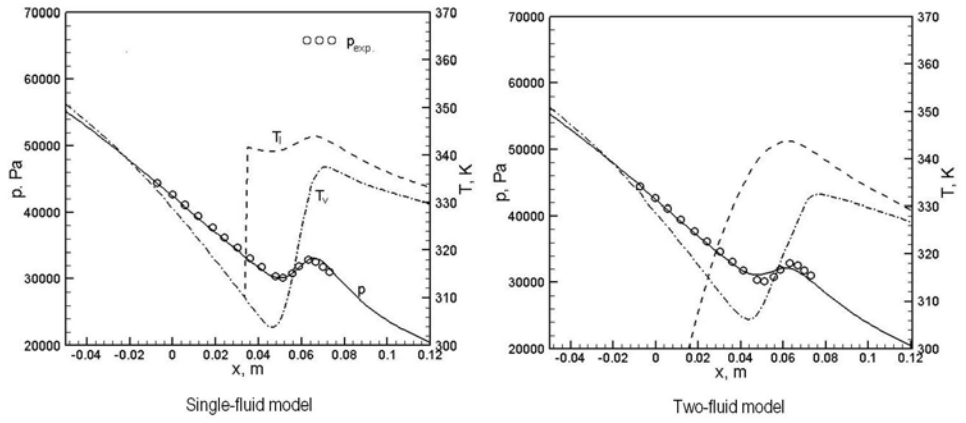

Figure 2. Pressure and temperature distributions along the nozzle.

by about 40% smaller than those measured in the experiment. In the case of the TFM, the droplets radii are bigger than in the SFM model (Fig. 3). The wetness fraction is similar in both models. The distributions of the nucleation rate and the number of droplets are presented in Fig. 4. The character of the nucleation rate follows from the differences in the condensation intensity for both models, weaker for the TFM.

The slip velocity modelled in the TFM model will depend on the flow

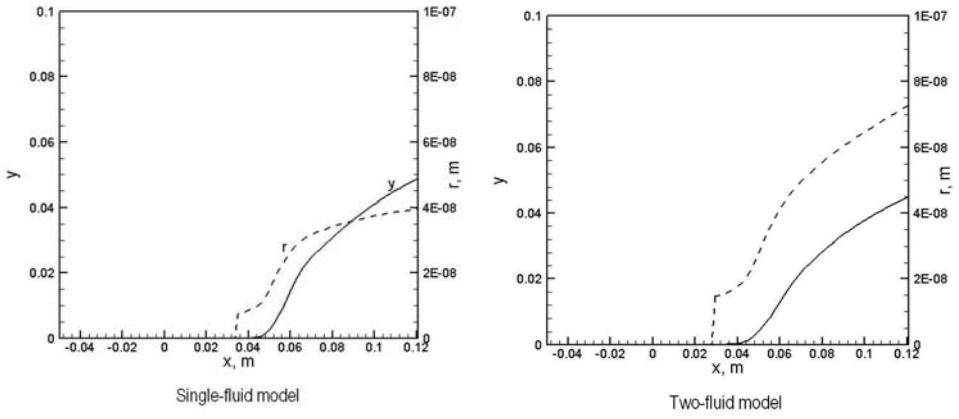

Figure 3. Wetness fraction and droplet radius distributions along the nozzle.

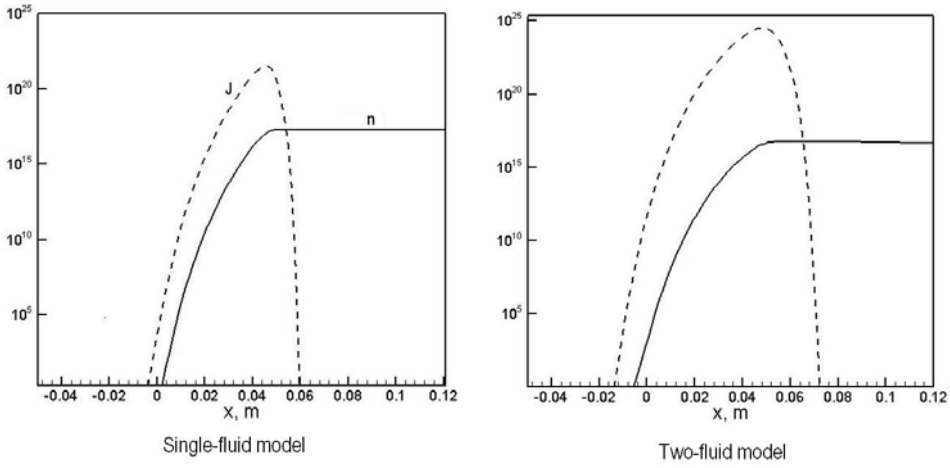

Figure 4. Distributions of nucleation rate and number of droplets along the nozzle.

pattern. In the case of the nozzle flow, the slip between the vapour and the liquid phase is the highest at the nozzle outlet close to the walls (Fig. 5).

4.2 Single-fluid model with homogeneous and heterogeneous condensation

The experiments of wet steam transonic flows are difficult mainly because of a problem with steam supply. The quality of steam has a great influence on

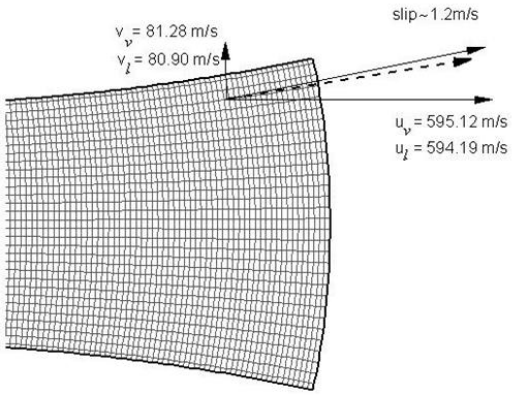

Figure 5. Slip of the velocities between vapour and liquid phase for TFM model.

the type of condensation process. If the steam was supplied directly from a steam power cycle or from industrial steam installation, the influence of impurities in condensation modelling has to be taken into account in experiment.

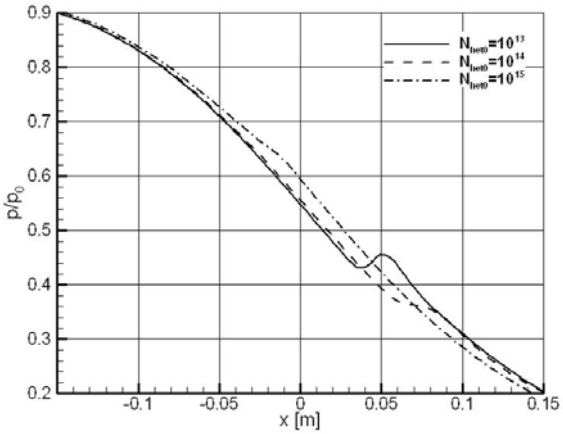

Figure 6. Effect of the insoluble particles concentration on the condensation process, $r_{p,het0} = 10^{-7}$ m.

We can notice from Figs. 6 and 7 that concentration of impurities in steam affects the condensation process significantly. Three concentrations of particles with radius 10^{-7} m were considered. The impurities extend the domain of the possible solutions and make the expansion process different. It shows

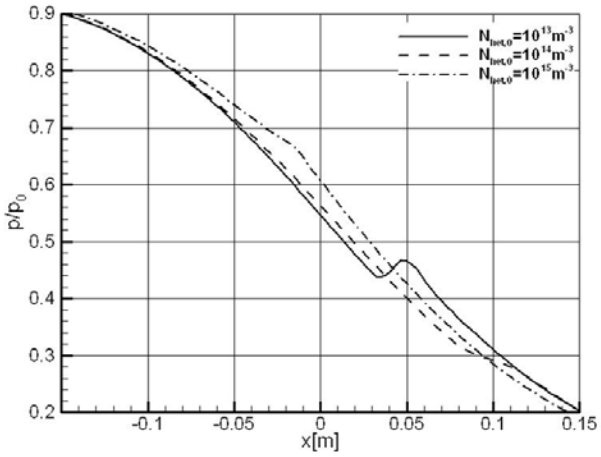

Figure 7. Effect of the soluble particles concentration on the condensation process, $r_{p,het0} = 10^{-7}$ m.

an importance of the steam quality data in validation of condensation models. The other parameters of impurities as particles mean radius and contact angle are important as well. Detailed description of these parameters can be found in [14].

5 Conclusions

The models presented in this paper and implemented into the in-house CFD code create the possibility to predict wet steam losses in LP turbine stages accurately. The results obtained show that both presented models, SFM and TFM, for the wet steam flow modeling can predict the place of condensation correctly in comparison with the experiment. The pressure and temperatures are similar. For the TFM, the predicted condensation wave is a little smoother than for the SFM; it is observed in the static pressure distributions. The wetness fraction is very similar, both in character and value. The SFM without special corrections mostly underestimates the droplet diameters. Consequently, the droplet radii obtained from the TFM, which are by approx. 40% bigger than in the calculations for the SFM model, show a better tendency. The velocity slip between the vapour and the liquid phase is observed in the TFM model, which shows the correct behavior of the applied drag forces. Therefore, by using the TFM in steam turbines, the thermodynamic and aerodynamic losses of the two-phase flow

can be predicted.

Two models of heterogeneous condensation on insoluble and soluble impurities are presented and discussed. The influence of impurities on expansion process was shown. The calculations of a steam condensing flow by means of the presented algorithms are very sensitive to the flow parameters that are dependent on state equation for vapour and liquid, Riemann problem solution, accuracy of integration in time and in space.

Acknowledgements The authors would like to thank the Polish Ministry for Science and Higher Education for the financial support within the Research Project 3341/B/T02/2010/38.

Received 3 January 2011

References

[1] Heiler M.: *Instationaere Phaenomene in homogen/heterogen kondensierenden Duesen- und Turbinenstroemungen*. PhD thesis, Universität Karlsruhe, Karlsruhe 1999.

[2] Dykas S.: *Numerical calculation of the steam condensing flow*. TASK Quarterly, Scientific Bulletin of Academic Computer Centre in Gdańsk **5**(2001), 4, 519-535.

[3] White A.J., Young J.B., Walters P.T.: *Experimental validation of condensing flow theory for a stationary cascade of steam turbine blade*. Philosophical Transaction of Royal Society London A **354**(1996), 59–88.

[4] Bakhtar F., White A.J., Mashmoushy H.: *Theoretical treatments of two-dimensional, two-phase flows of steam and comparison with cascade measurements*. Proc. of the Institution of Mechanical Engineers, Part C, J. Mechanical Engineering Science **219**(2005), 1335–1355.

[5] Karkoszka K., Anglart H.: *CFD modelling of laminar film and spontaneous condensation in presence of noncondensable gas*. Archives of Thermodynamics **27** (2006), 2, 23–36.

[6] Dykas S., Wróblewski W., Lukowicz H.: *Prediction of losses in the flow through the last stage of low pressure steam turbine*. Int. J. Numer. Meth. Fluids **53**(2007), 933–945.

[7] Wróblewski W., Dykas S., Gardzilewicz A., Kolovratnik M.: *Numerical and experimental investigations of steam condensation in LP part of a large power turbine*. Trans. ASME J. Fluids Eng. **131**(2009), 4, 041301.

[8] Frenkel J.: *Kinetic Theory of Liquids.*, Oxford University Press, New York 1946.

[9] Gyarmathy G.: *Grunglagen einer Theorie der Nassdampfturbine*. PhD. thesis, Juris Verlag, Zürich 1960.

[10] Kantrowitz A.: *Nucleation in very rapid vapour expansions.* J. Chemical Physics **19**(1951), 1097–1100.

[11] Gorbunov B., Hamiltion R.: *Water nucleation on aerosol particles containing both soluble and insoluble substances.* J. Aerosol Sci. **28**(1997), 2, 239-248.

[12] Barschdorff D.: *Verlauf der Zustandsgrossen und gasdynamische Zusammenhange der spontanen Kondensation reinen Wasserdampfes in Lavalduesen.* Forschung im Ingenieurwesen **37**(1971), 5, 146–157.

[13] Wróblewski W., Dykas S., Gepert A.: *Steam condensing flow in turbine channels.* Int. J. Multiphase Flow **35**(2009), 6, 498–506.

[14] Wróblewski W., Dykas S., Gepert A.: *Modelling Water Vapour Flow with Heterogeneous Condensation.* Wydawnictwo Politechniki Śląskiej. Gliwice 2006 (in Polish).